

Measuring the quantum state of an electromagnetic field using the atomic Talbot effect

B. Rohwedder, L. Davidovich, and N. Zagury

Instituto de Física, Universidade Federal do Rio de Janeiro, Caixa Postal 68.528, 21945-970 Rio de Janeiro, RJ, Brazil

(Received 3 December 1998)

Fractional Talbot images in the de Broglie near field of atoms diffracted by a dispersive light grating allow the measurement of the quantum state of an electromagnetic field in a cavity, in the optical domain. In particular, the photon-number statistics may be obtained, in principle, through a single experimental realization. It may be expressed as a Fourier transform of the atomic density on a plane situated at one-fourth of the Talbot distance from the light grating. The proposed measurement of the density matrix of a standing light wave using “Talbot fingerprints” should be feasible within the present state of the art.
[S1050-2947(99)02407-5]

PACS number(s): 03.75.Be, 32.80.-t, 42.50.-p

I. INTRODUCTION

The oldest observation of what is now called the “Talbot effect” was described in 1836 [1], at a time when the wave description of light was still called “the undulatory hypothesis” in England. This effect can be observed in the near field of a plane wave diffracted by a periodic structure, and is associated with a first-order correction beyond ray optics. One should expect that, due to diffraction effects, simple geometrical shadows of the periodic structure get replaced, in the near-field region, by more complex images. However, at entire multiples of a fundamental length D , exact shadows (“Talbot images”) of the grating show up. The length D , commonly referred to as the “Talbot distance,” is expressed in terms of the grating period d and the wavelength λ of the incident radiation by $D = 2d^2/\lambda$. The waves exhibit therefore a periodicity along the propagation direction, after crossing the grating. The first theoretical explanation of this effect was given by Rayleigh in 1881 [2]. A historical review can be found in [3]. Recent theoretical studies in the context of atom optics can be found in [4–7].

The Talbot effect has been applied to the comparison of diffraction gratings, in situations where it is not desirable to directly superimpose them. The direct superposition method was used by Lord Rayleigh, who tested optical gratings by observing the arising Moiré pattern [8]. Instead of using the “true” shadow, as was done in the superposition method, one can alternatively use the Talbot self-images that appear at integral multiples of the Talbot distance (or its half) to test diffraction gratings. This is especially useful for fragile gratings, since it would avoid the mechanical contact between them. This method was preferred in Ref. [9], where very fragile, 200 nm and 300 nm period gratings were tested using sodium atoms. At the same time, this experiment constituted a nice demonstration of the Talbot effect with atomic matter waves. Several other experiments also demonstrated the Talbot effect with atom waves, using amplitude gratings [10]. Recently, the virtues of a novel atom detector with high spatial resolution have been demonstrated by using it to depict Talbot fringe patterns at various distances behind a micro-fabricated structure with a comparatively large grating constant of $6.55 \mu\text{m}$ [11]. For finer gratings a direct measurement of the atomic density distribution in the near field

becomes increasingly difficult, since detectors with the required spatial resolution cannot be easily implemented. This problem can be circumvented with the help of a second grating of equal period: by laterally scanning this “mask” while measuring the proportion of transmitted atoms, detailed pictures of the Talbot near field can be obtained. The shape of the more complex images that appear at fractions of the Talbot distance can also be determined this way, as long as the open fraction of the “probe” grating is chosen small enough. A beautiful example can be found in Ref. [12], where the diffraction of argon atoms by a novel type of absorptive “quenching-effect” grating made of light (grating constant 400 nm) is demonstrated [13].

To the best of our knowledge, the Talbot effect has never been confirmed with atoms crossing a strongly detuned standing light field, even though the experimental parameters used to observe far-field diffraction in such a configuration [14] are ideally suited for demonstrating this near-field effect as well. Due to the governing dispersive interaction, such a structure plays the role of a sinusoidal phase grating for atomic de Broglie waves.

The Talbot effect with phase gratings has been considered before, for electromagnetic waves. As the waves propagate in free space behind the grating, the initially pure phase modulation eventually gets transformed into a pure amplitude modulation at one-fourth of the Talbot distance [15].

The attractiveness of atom-optics gratings based on standing electromagnetic waves comes from the ease of calibration of these devices, by changing the field intensity and the cavity length. However, in the regime of low intensities, one must pay attention to the quantum nature of the field involved. It is the purpose of the present paper to include the quantum properties of the field in the Talbot effect for atomic waves, and to show that the near-field diffraction pattern at this particular distance $D/4$ is highly sensitive to the quantum field statistics of the diffracting light field. In fact, we will show that under certain conditions the fractional Talbot image at $D/4$ represents a one-to-one mapping of the photon-number distribution, and that its inversion is very simple, allowing in principle the full determination of the photon-number distribution of the field through the measurement of the atomic density on the $D/4$ plane. This is a quantum nondemolition measurement, since the dispersive inter-

action between the atoms and the field does not change the photon-number distribution. We also show that, by injecting a coherent state into the cavity containing the field to be measured, one can determine from the atomic distribution the Wigner function of the initial field at any point of phase space.

As we will show, our method may have some advantages with respect to other procedures proposed so far for state reconstruction of optical fields in cavities, and transforms the striking Talbot effect into a useful tool for quantum state diagnosis of a standing-wave light field. A series of different schemes for this purpose are given in Refs. [16–23]. Closest to our proposal are the methods discussed in Refs. [20,22] which also consider two-level atoms in their ground state interacting dispersively with a standing light field in a cavity. Contrary to our scheme, in which it is of central importance that the atoms “see” many nodes of the standing wave, these techniques require atoms to cross only a small section of the optical potential. This obliges one to restrict the atomic motion by using appropriate slits. Our approach does not require any such additional and flux-reducing structures, because it makes actual use of the periodicity of the optical potential from the very beginning.

Also, our proposal differs from those in Refs. [17,19] in an essential way. In our method the information on the photon-number statistics can be easily obtained, in principle, after a single realization, from the probability density of finding the atoms in each position of a plane parallel to the standing-wave grating. In the quantum nondemolition (QND) procedures proposed in Refs. [17,19], this information is obtained after several realizations, the field being projected, in each realization, onto a Fock state by the successive detection of the atoms which cross the field grating. Consideration of the near-field region not only leads to analytical expressions for the field statistics in terms of the atomic distribution, which allow the reconstruction of the field statistics after a single realization, but one also benefits from the redundancy associated with the periodicity of the atomic position pattern.

The proposition presented in [23] is similar to ours in the sense that a one-to-one mapping of a cavity state on an atomic degree of freedom is performed. While we use the motional state to perform this mapping, the internal atomic structure is employed in that reference. Specifically, the quantum state of the field is impinged on an atomic Zeeman submanifold via an adiabatic transition. A subsequent series of Stern-Gerlach measurements is used to retrieve the stored information from a series of identically prepared atoms. This beautiful idea does not require atom detectors with high spatial resolution as in our scheme. On the other hand, it is limited to atoms with an adequate level structure, and it requires an additional laser and external magnetic fields. Also its mathematical description is substantially more complex than in our case.

Finally, Refs. [16,18,21] are based on resonant interactions and thus do not represent QND measurements. Because each atom changes the field population to be measured, these proposals also require rebuilding the initial field after each atom is measured.

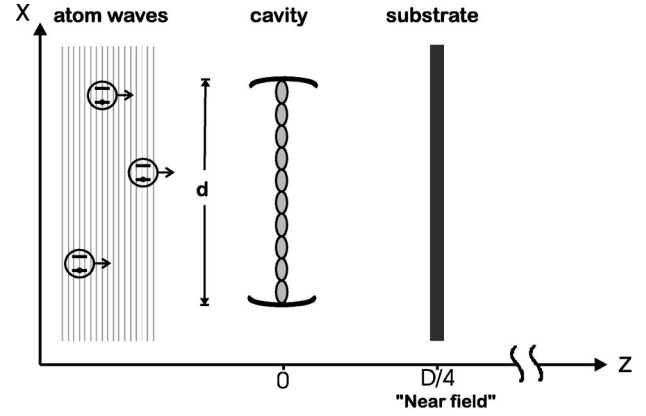


FIG. 1. Two-level atoms coming from the left interact with the field in the cavity and are detected on a substrate at $z = D/4$.

II. THE ATOMIC TALBOT EFFECT

We consider here a one-mode standing optical field, periodic along the x axis, crossed by an orthogonal atomic beam, which propagates along the z axis, as schematically shown in Fig. 1. We assume, for the sake of simplicity, that the field as well as the atomic beam are uniform along the y direction, and that the amplitude of the light field is constant along the z direction, being confined in the region $-L < z < 0$. Some of these conditions will be relaxed later on. The atoms are prepared in the ground state, and we assume that the detuning between the field frequency and the atomic transition frequencies is sufficiently large so that transitions from the ground state can be safely neglected. Only the closest-tuned excited state needs to be considered, and the atom can be taken as a two-level atom. This requires that $|G|^2 n \ll \Delta^2 + \gamma^2$, where G is the amplitude of the x -dependent single-photon Rabi frequency

$$g(x) = G \sin\left(\frac{2\pi x}{\lambda}\right), \quad (1)$$

n is the characteristic photon number, Δ is the detuning of the field from the two-level transition frequency (without loss of generality we assume $\Delta > 0$ for notational simplicity), and γ is the spontaneous emission rate from the excited state. We also assume that the number of spontaneously emitted photons in the interaction region is very small, which implies that $|G|^2 n \gamma t_{\text{int}} / (\Delta^2 + \gamma^2) \ll 1$, where t_{int} is the interaction time. Under these conditions, and assuming also that $\Delta \gg \gamma$, the interaction can be written as

$$H_{\text{eff}} = \frac{\hbar |g(x)|^2}{\Delta} \sigma_z a^\dagger a. \quad (2)$$

Here the operators a and a^\dagger , with $[a, a^\dagger] = 1$, are the annihilation and creation operators corresponding to the standing-wave field mode of frequency $\omega = 2\pi c/\lambda$, and $\sigma_z = |+\rangle\langle+| - |-\rangle\langle-|$, where $|+\rangle$ and $|-\rangle$ refer to the upper and lower atomic states, respectively.

Furthermore, we assume that the standing wave constitutes a thin optical medium, so that the transverse kinetic energy absorbed by the atom during the interaction is much

smaller than the dispersive atom-field coupling. This is known as the Raman-Nath regime [24]. For the standing-wave interaction given by Eq. (2), the variation of the kinetic energy along x , due to the gradient force dH_{eff}/dx , will be of the order of $(|dH_{\text{eff}}/dx|t_{\text{int}})^2/2M \sim (\hbar kt_{\text{int}})^2 G^4 n^2/2M\Delta^2$, where M is the atomic mass, and $k=2\pi/\lambda$. Therefore, the Raman-Nath regime requires that $\hbar(kGt_{\text{int}})^2 n/M\Delta \ll 1$. This same condition guarantees that the total displacement of the atom along the x axis in the interaction region is much smaller than the wavelength of the standing wave. The light field becomes then a pure phase grating for the atomic waves, described by the effective interaction (2). Also, since the atoms will remain in their lower level $|-\rangle$ all the time, one does not need to take the internal degrees of freedom into account. For thermal atomic velocities, the kinetic energy associated with the atomic motion along the z axis is much larger than the amplitude of the dispersive interaction, so that the reflection of the atomic beam on the standing wave is negligible. We assume that the field is described by a density operator ρ , with a photon-number distribution given by $p_n = \langle n|\rho|n\rangle$.

The initial plane atomic wave, normalized to unity density, enters the light field at $t = -t_{\text{int}}$. In the Raman-Nath regime considered here, the light field simply acts as a pure phase grating, thus producing, at its exit, and if there are n photons in the field,

$$\psi_n(x,0) = e^{in\phi \sin^2(2\pi x/\lambda)}, \quad (3)$$

where $\phi = G^2 t_{\text{int}}/\Delta$. Free propagation then leads to

$$\begin{aligned} \psi_n(x,t) = & \sqrt{\frac{M}{i2\pi\hbar t}} \int_{-\infty}^{\infty} dx' e^{(i/\hbar)(M/2t)(x')^2} \\ & \times e^{in\phi \sin^2[2\pi(x'+x)/\lambda]} \end{aligned} \quad (4)$$

behind the grating.

We introduce now the natural variables X and Z , defined by

$$x \equiv \frac{\lambda}{2} \frac{X}{2\pi}, \quad z = v_z t \equiv D \frac{Z}{2\pi}, \quad (5)$$

where $D \equiv 2(\lambda/2)^2/(h/Mv_z)$ is the Talbot distance, v_z is the velocity of the atomic beam in the z direction, and $\lambda/2$ is the period of the intensity grating. Atom detectors allow the measurement of the probability density distribution corresponding to Eq. (4), which can be expressed in terms of a Fourier series expansion [25]:

$$|\psi_n(x,t)|^2 = \sum_{j=-\infty}^{\infty} e^{ijX} J_j[-n\phi \sin(jZ)], \quad (6)$$

where J_j is a Bessel function. In this form it becomes evident that the diffraction pattern is not only periodic along the grating axis X but also along the propagation axis Z . Equation (6) thus defines a doubly periodic function in the X - Z plane. Although this is not evident from Eq. (4), the same statement applies to the wave amplitude itself. That is the essence of the so-called Talbot effect.

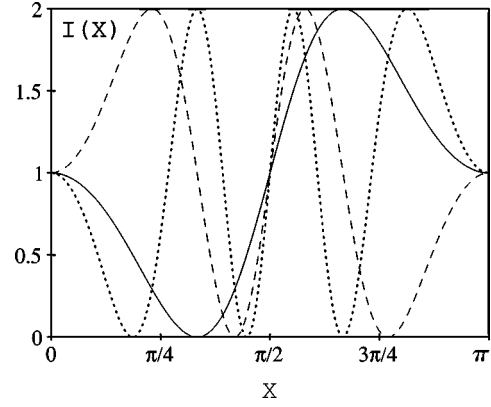


FIG. 2. Density distribution of atoms scattered by a light field in the number states $n=1$ (solid line), $n=2$ (dashed line), and $n=3$ (dotted line). $z=D/4$, $G^2 t_{\text{int}}/\Delta = \pi$.

III. PHOTON STATISTICS AND WIGNER FUNCTION

In the strong coupling regime it is nowadays possible to achieve values of ϕ larger than unity. Figure 2 depicts the density distribution of atoms scattered by a light field in the number states $n=1$, $n=2$, and $n=3$, respectively, at $z=D/4$, when $\phi = \pi$ is assumed. It is evident from these pictures that in this regime near-field imaging becomes strongly dependent on the governing field statistics. The natural question arises, if it is also possible to unambiguously read off the field photon statistics from the Talbot pattern it produces. That this question is not trivial can be inferred from the fact that the intensity distribution observed, for instance, at the Talbot distance D or its half is just constant and thus provides no information about the electromagnetic field. We will show, however, that the fractional Talbot image at $D/4$ contains the full information needed.

Indeed, at $Z/2\pi = 1/4$ (that is, $z=D/4$), Eq. (6) reduces to

$$|\psi_n(x,t)|^2 = 1 - \sin(n\phi \cos X). \quad (7)$$

If instead of a Fock state one has a photon-number distribution p_n , the intensity I measured by the detector, normalized so that $I=1$ if there is no field in the cavity, is given by the superposition

$$I(X) \equiv 1 - \sum_{n=1}^{\infty} p_n \sin(n\phi \cos X). \quad (8)$$

If $\phi \geq \pi$, it is straightforward to show, using the Fourier theorem, that the coefficients p_n ($n > 0$) are given by

$$p_n = \frac{2\phi}{\pi} \int_a^b dX \sin X \sin(n\phi \cos X) [1 - I(X)], \quad (9)$$

with $a = \cos^{-1}(\pi/\phi)$ and $b = \cos^{-1}(0)$, while $p_0 = 1 - \sum_{n=1}^{\infty} p_n$. Equation (9) shows that the photon-number distribution can be obtained in a very simple way from the atomic distribution. This result is a peculiarity of the near field. In the far field there does not seem to exist a simple analog to Eq. (9) for the retrieval of information on the photon-number distribution of the electromagnetic field.

It is easy to see why p_0 cannot be obtained directly from the atomic distribution: the atomic wave function is not changed if there are no photons in the cavity. The periodic structure of $I(X)$ allows the above integration to be replaced

by an average over many periods of the atomic distribution, thus enhancing the information content of the measured data.

The restriction $\phi = G^2 t_{\text{int}} / \Delta \geq \pi$ has a simple physical meaning: a small coupling term implies that only weak distortions of the initially plane de Broglie wave front will take place. Contributions corresponding to different photon numbers are then virtually indiscernible for small n . This condition is compatible with recent experimental data. In a high-finesse optical cavity coupling constants as high as $G/2\pi = 120$ MHz have already been achieved [26] (one should remark, however, that the particular setup described in that reference is not useful for our purpose: the pronounced non-uniformity of the field distribution in the cavity used by those authors prevents the realization of a phase grating with the needed periodicity). In order to get $G^2 t_{\text{int}} / \Delta > \pi$, for an interaction time $t_{\text{int}} \approx 100$ ns, and $\Delta \approx 10G\sqrt{n}$ and $n \approx 1$ it is sufficient to have $G/2\pi > 50$ MHz. Typical values for one-fourth of the Talbot distance are in the millimeter range (if $\lambda = 500$ nm and $\lambda_{dB} = 0.2$ Å we get $D \approx 1$ cm). One should note that if $\phi \gg \pi$ the Talbot pattern oscillates very fast, rendering more difficult the application of this method. Therefore one should have ideally $\phi \sim \pi$.

We show now how to extract from the fractional Talbot image at $z = D/4$ complete information about the state of the electromagnetic field, through the measurement of its Wigner representation. The Wigner quasiprobability distribution $W(\alpha)$ corresponding to the standing-wave field allows the calculation of symmetrically ordered products of field operators as classical-like phase-space integrals, with the operators a and a^\dagger replaced by the c -numbers α and α^* , respectively [27]. It completely characterizes the quantum state of the field, and can be obtained from the formula [27,29]

$$W(\alpha) = \frac{2}{\pi} \sum_{n=0}^{\infty} (-1)^n p_n(-\alpha), \quad (10)$$

where $p_n(-\alpha)$ is the photon-number distribution of the field obtained by coupling the cavity to a classical source that displaces the original field in phase space by the complex amplitude $-\alpha$ [28] (this can be implemented by injecting light from a well-stabilized laser, working sufficiently above threshold; the whole experiment must be done during a time much smaller than the coherence time of the laser). The normalization in Eq. (10) is chosen so that $\int d^2\alpha W(\alpha) = 1$, where $d^2\alpha$ stands for $d(\text{Re } \alpha)d(\text{Im } \alpha)$. We note that the same expression was used to determine the Wigner distribution corresponding to the center-of-mass motion of a trapped ion at NIST [29] and of atoms diffracted from a Young double slit in Konstanz [30]. A similar procedure, proposed for microwave fields [31], involves the measurement of internal states of two-level atoms which cross the cavity field, after a displacement in phase space. In our case, however, it is possible to directly express the Wigner function in terms of the atomic center-of-mass distribution. Indeed, from Eqs. (9) and (10), and the expression for p_0 , it is easy to show that, if $I_{-\alpha}(X)$ is the atomic distribution after the phase-space displacement of the original field by $-\alpha$, then

$$W(\alpha) = \frac{2}{\pi} \left\{ 1 + \frac{2\phi}{\pi} \int_a^b dX \frac{[1 - I_{-\alpha}(X)] \sin X}{\sin(\phi \cos X)} \right\}. \quad (11)$$

This equation expresses the Wigner function of the cavity field in terms of the atomic distribution on a plane situated at one-fourth of the Talbot distance from the standing-wave grating. One should note that the integrand is not singular at $X = \pi/2$: it follows indeed from Eq. (8) that for this value of X it converges to $\langle n \rangle$.

In practice, in order to measure the Wigner function at a point α of phase space, one would displace the field to be measured by $-\alpha$, and then send the atoms across the field, measuring their distribution on a plane at the proper position. A detector with high ($\ll \lambda/2$) spatial resolution is needed for this experiment. The deposition of the atoms on a substrate is a viable method. The deposited structure can be observed either with scanning probe techniques [32] or in real time by optical diffraction [33]. Although the intrinsic size of the atoms, their mobility on the surface, and shot noise due to their finite number set basic physical limits to the method, there is also a big advantage: all the information is stored on a stripe of finite width and, due to the periodicity of the deposited atom layer, there is a high amount of redundancy in the information content, which can be made use of by averaging over many periods.

It is interesting to compare the above procedure with the far-field version of this experiment. The corresponding basic expression may be obtained by expanding the sinusoidal phase factor in Eq. (4) in terms of plane waves, using the generating identity for Bessel's functions $J_j(\alpha)$,

$$e^{ia \sin k} = \sum_{j=-\infty}^{\infty} J_j(a) e^{ijk}, \quad (12)$$

and considering the free propagation to the far-field region, one gets the well-known expression for the j th-order diffraction intensity [14]:

$$\frac{I_j}{I} = \sum_{n=0}^{\infty} p_n J_j^2 \left(n \frac{G^2 T}{2\Delta} \right). \quad (13)$$

One should note, as mentioned before, that an inversion formula like Eq. (9) does not seem to exist in the far-field region.

IV. ABERRATION EFFECTS

In any real experiment the assumptions which led to the above model can only be satisfied in an approximate manner. Departures from the expected behavior may be caused by a series of effects that strongly depend on the specific experimental conditions. In this section we discuss the influence of some sources of aberrations on the quality of the proposed QND measurement.

A. Finite aperture

We have assumed that a plane wave reaches the cavity field at time $t = -t_{\text{int}}$. Collimating slits in the atom beam, the limited size of the physical cavity, and the Gaussian waist dimensions of a typical electromagnetic mode, however, naturally define a *finite* entrance aperture a of the system and give rise to the distinction of a near and a far field. The question of how much the Talbot images are distorted due to an entrance pupil has been repeatedly addressed in the litera-

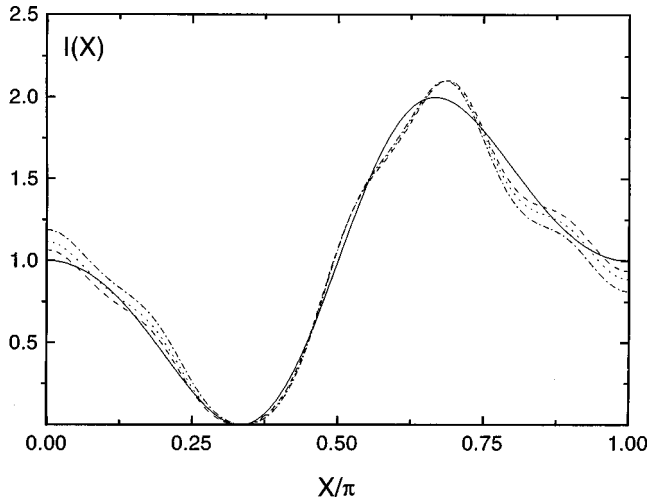


FIG. 3. Intensity $I(X)$ at $z=D/4$ for (a) infinite aperture (solid line); (b) $a=10\lambda$, $\eta=0$ (dashed line); (c) $a=10\lambda$, $\eta=0.04$ (dotted line); (d) $a=10\lambda$, $\eta=0.10$ (dash-dotted line).

ture [3]. A quite general approach is given in Ref. [34]. Here we prefer to numerically compare the idealized near-field image (7) at $z=D/4$ with its aperture-limited counterpart. Under the assumption of a rectangular entrance slit profile, the condition

$$\frac{D}{4} \ll \frac{a^2}{h/Mv_z} \quad (14)$$

for the observation plane to be in the near field is very well fulfilled. Indeed, this condition does not depend on the atomic momentum, but only on the grating period/aperture ratio, as $(\lambda/2)^2 \ll 2a^2$. Figure 3 shows the results for the intensity as a function of X when there is a Fock state with $n=1$ inside the cavity and the size of the aperture is $a=10\lambda$. One can see that the distortions in the intensity are quite small (dashed line) as compared with the results of Sec. III of this paper (solid line) and should not affect very much the determination of p_n even when only 20 grating periods are illuminated.

B. Gaussian cavity mode profiles

Another source of distortions comes from the geometry of the cavity, and manifests itself in two ways. First, the standing electromagnetic wave has a transverse dependence, which we simulate through an X dependence of the form $w(X) = w_0 \{ [1 + \eta(X/a)^2] \}^{1/2}$, which is typical of a Gaussian mode of a resonator [35]. The dotted and the dash-dotted lines in Fig. 3 represent the situation where $a=10\lambda$ and when $\eta=0.04$ and $\eta=0.10$, respectively. As we can see in the figure, the discrepancies with the results for $I(X)$ obtained in Sec. II are quite small.

Furthermore, the electromagnetic mode is not flat topped, since sharp edges are never realized in actual experiments. The turning on of the coupling (1) may be modeled by some smooth function f that describes the cross-sectional shape of the laser beam

$$g(x, z=v_z t) = f(t) G \sin\left(\frac{2\pi x}{\lambda}\right). \quad (15)$$

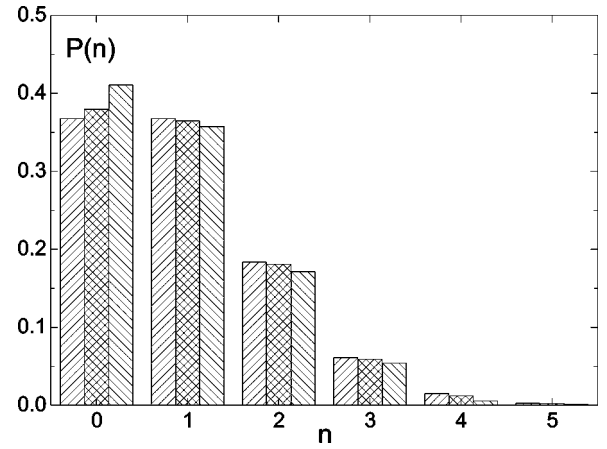


FIG. 4. Simulation of photon distribution for a coherent state with $\bar{n}=1$ when the velocity distribution is Gaussian, with variance Δv_z . For each value of n , the three columns represent, from left to right, the photon statistics for the original field distribution, and the distributions for $\Delta v_z = 0.01 \bar{v}_z$ and $\Delta v_z = 0.02 \bar{v}_z$. $G^2 \bar{t}_{\text{int}} / \Delta = \pi$. p_0 is obtained from $p_0 = 1 - \sum_{n=1}^{\infty} p_n$.

One easily shows, in the same way as in Ref. [36], that our results remain true for any f , as long as the turning on is adiabatic and the time variable t is replaced by $\tau = \int dt f^2(t)$. Thus, by changing the parametrizations of time accordingly and making sure that the region of interest ($z=D/4$) is well outside the interaction area, the two descriptions essentially coincide.

C. Chromatic aberration

The Talbot effect depends strongly on the wavelength. It is thus mandatory to study how much the velocity distribution in a realistic atom beam distorts the near-field intensity distribution. For this purpose we have made a series of numerical simulations using a Gaussian distribution of velocities. We find that, as long as the mean photon number of the field is not too high, longitudinal velocity dispersions as high as a few percent do not change appreciably the values obtained for the photon statistics and the Wigner function from Eqs. (9) and (10). In Figs. 4 and 5 we show, as an example, the results obtained for the photon distribution for a coherent state and a cross section ($\text{Re } \alpha > 0, \text{Im } \alpha = 0$) of the Wigner function for a Fock state with $\bar{n}=1$, when we consider dispersions of 1% and 2% of the mean longitudinal velocity. We observe that the measurement is only minimally deteriorated when such rather moderate longitudinal velocity spreads are assumed [the value shown for p_0 is calculated from $p_0 = 1 - \sum_{n=1}^{\infty} p(n)$ and therefore accumulates the errors in the determination of all $p(n)$].

D. Transverse incoherence

The required lateral coherence of the atomic wave front will usually be achieved with a collimating slit [9], very much like in Talbot's seminal work [1]. As noted in both these references, a narrower slit produces better imaging since it represents a more accurate realization of a point source. In such a configuration, our assumption of a plane atomic wave front at the grating plane is only approximately

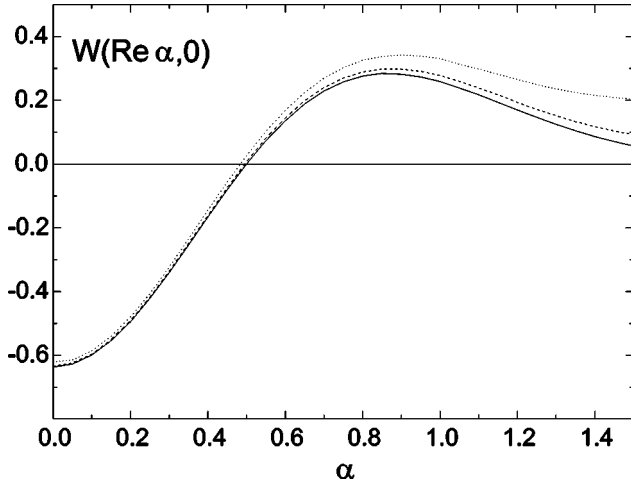


FIG. 5. Simulations for a cross section of the Wigner distribution when the velocity distribution is Gaussian. The solid line represents the true Wigner function for a Fock state with $n=1$, while the dashed and the dotted lines are simulations for $\Delta v_z = 0.01\bar{v}_z$ and $\Delta v_z = 0.02\bar{v}_z$. $G^2 t_{\text{int}}/\Delta = \pi$.

fulfilled. It is well known, however, that a wave front of constant curvature keeps the form of the Talbot images intact and only amounts to a shadowlike magnification of their size, proportional to the distance away from the grating [3], and to which our measurement scheme is insensitive. With no loss of generality, we will thus retain our initial, plane wave illumination assumption. Lateral incoherence may then be modeled by adding the intensities (not the amplitudes) of the near-field diffraction patterns produced by paraxial plane waves which cross the light grating at different angles. This oblique incidence is described by initial lateral velocities $v_x \neq 0$.

When considering fluctuations around $v_x = 0$, the change in the interaction time t_{int} due to the nonorthogonal incidence on the light mode can be completely neglected due to $\Delta v_x/v_z \ll 1$ for any realistic beam. On the contrary, the lateral displacement of the quarter Talbot image is independent of v_z and thus highly sensitive to variations in v_x . If we are able to maintain the variance Δv_x smaller than the one-photon recoil velocity the errors in the determination of the photon statistics and the Wigner function are not too large, as is shown in Figs. 6 and 7. If this is not the case, it is still possible, in principle, to retrieve the true Wigner function if the velocity distribution is known, since the process is coherent. Let us exemplify this procedure in the case of a typical, Gaussian velocity distribution. Let

$$B(X) = \frac{1}{\sqrt{2\pi}\sigma} \int_{-\infty}^{\infty} dX' e^{-(1/2)[(X'-X)/\sigma]^2} I(X') \quad (16)$$

be the blurred image to be deconvoluted. The rationalized distribution width σ is measured in units of photon momentum, i.e.,

$$\sigma = \frac{1}{4} \frac{M\Delta v_x}{h/\lambda}. \quad (17)$$

By expanding both B and I into Fourier series,

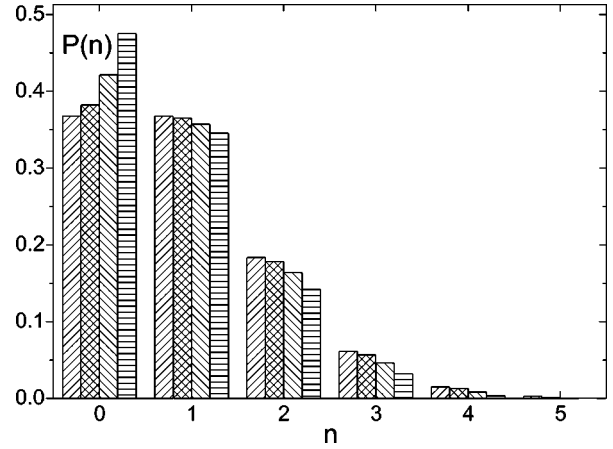


FIG. 6. Simulation of photon distribution when the transverse velocity is Gaussian with variance Δv_x , for a coherent state with $\bar{n}=1$. For each value of n , the four columns represent, from left to right, the original field distribution, and the distributions for $M\Delta v_x$ equal to $0.025h/\lambda$, $0.050h/\lambda$, and $0.10h/\lambda$. $G^2 t_{\text{int}}/\Delta = \pi$. p_0 is obtained from $p_0 = 1 - \sum_{n=1}^{\infty} p_n$.

$$B(X) = \sum_{j=-\infty}^{\infty} B_j e^{iXj}, \quad I(X) = \sum_{j=-\infty}^{\infty} I_j e^{iXj}, \quad (18)$$

one finds, after reinsertion into Eq. (16), that the Fourier coefficients B_j and I_j are related through

$$I_j = B_j e^{(\sigma^2/2)j^2}. \quad (19)$$

In an experiment, one would probably deal directly with the Fourier components of B as read off from the deposited atom layer. Inasmuch as higher coefficients fall off exponentially with σ^2 , the velocity distribution width should not be too broad. Nonetheless, the actual limitation on σ is not given by the photon-recoil velocity but depends only on the ability to resolve higher spatial frequencies in B . Formally, one can express I directly in terms of B by resumming the series (18). The inverse of Eq. (16) then reads

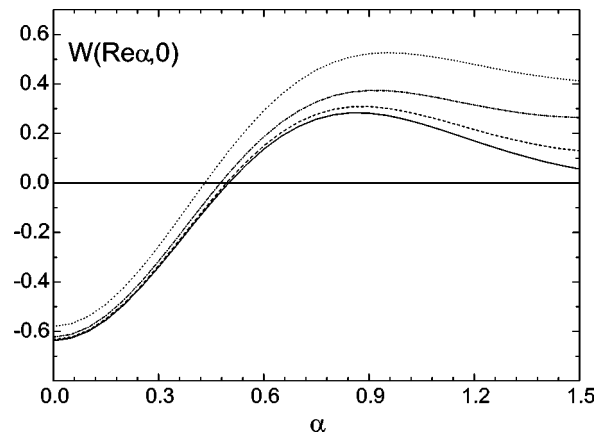


FIG. 7. Simulations for a cross section of the Wigner distribution when the velocity distribution is Gaussian. The solid line represents the true Wigner function for a Fock state with $n=1$, while the dashed, dash-dotted, and dotted lines are simulations for $M\Delta v_x$ equal to $0.025h/\lambda$, $0.050h/\lambda$, and $0.10h/\lambda$. $G^2 t_{\text{int}}/\Delta = \pi$.

$$I(X) = \exp\left\{-\frac{\sigma^2}{2}\left(\frac{d}{dX}\right)^2\right\}B(X). \quad (20)$$

V. CONCLUSIONS

We have considered in this paper the near-field diffraction pattern of atomic beams which interact dispersively with a standing electromagnetic wave, taking into account the quantum structure of the electromagnetic field. We have shown that the Talbot effect is highly sensitive to the quantum statistics of the field. Based on this remark, we have proposed a scheme for the measurement of the quantum state of optical fields in cavities using Talbot “fingerprints,” in which the structure of the de Broglie near field of atoms diffracted by a light grating is used to determine the photon-number distri-

bution and the Wigner function of the field in the cavity. Our method does not require successive reinitializations of the experiment: in principle, a single realization allows the reconstruction of the quantum state of the field.

ACKNOWLEDGMENTS

The authors acknowledge fruitful discussions with C. Lenz Cesar, and thank M. S. Chapman for bringing Ref. [26] to their attention. This work was supported by FONDECYT Grant No. 2950068, the Conselho Nacional de Desenvolvimento Científico e Tecnológico (CNPq), the Latin American Center for Physics (CLAF), and the Programa de Apoio a Núcleos de Excelência (PRONEX).

-
- [1] W. H. Fox Talbot, *Philos. Mag.* **9**, 401 (1836).
 [2] L. Rayleigh, *Philos. Mag.* **11**, 196 (1881).
 [3] K. Patorski, in *Progress in Optics*, edited by E. Wolf (North-Holland, Amsterdam, 1989), Vol. 27.
 [4] J. F. Clauser and M. W. Reinsch, *Appl. Phys. B: Photophys. Laser Chem.* **54**, 380 (1992).
 [5] U. Janicke and M. Wilkens, *J. Phys. II* **4**, 1975 (1994).
 [6] O. Carnal, Q. A. Turchette, and H. J. Kimble, *Phys. Rev. A* **51**, 3079 (1995).
 [7] See the corresponding articles in *Atom Interferometry*, edited by P. R. Berman (Academic, New York, 1997).
 [8] A discussion of Moiré fringe patterns, their relation to the Talbot effect, and a list of common applications can be found in A. W. Lohmann and D. E. Silva, *Opt. Commun.* **2**, 413 (1971).
 [9] M. S. Chapman, C. R. Ekstrom, T. D. Hammond, J. Schmiedmayer, B. E. Tannian, S. Wehinger, and D. E. Pritchard, *Phys. Rev. A* **51**, R14 (1995).
 [10] The appearance of Talbot self-images depends crucially on the spatial coherence properties of the source. Interestingly, a related phenomenon can be observed using incoherent sources, as long as a further grating with small open fraction (“periodic point source”) is placed in front of the grating under study. This so-called Lau effect was demonstrated with potassium atoms and a coarse (8.1 μm) microfabricated grating in J. F. Clauser and S. Li, *Phys. Rev. A* **49**, R2213 (1994).
 [11] S. Nowak, Ch. Kurtsiefer, T. Pfau, and C. David, *Opt. Lett.* **22**, 1430 (1997).
 [12] R. Abfalterer, C. Keller, S. Bernet, M. K. Oberthaler, J. Schmiedmayer, and A. Zeilinger, *Phys. Rev. A* **56**, R4365 (1997).
 [13] K. S. Johnson, J. H. Thywissen, N. H. Dekker, K. K. Berggren, A. P. Chu, R. Younkin, and M. Prentiss, *Science* **280**, 1583 (1998).
 [14] P. L. Gould, G. A. Ruff, and D. E. Pritchard, *Phys. Rev. Lett.* **56**, 827 (1986).
 [15] P. R. Pisharoty, *Proc.-Indian Acad. Sci., Sect. A* **4**, 27 (1936); N. S. N. Nath, *ibid.* **4**, 262 (1936); S. Parthasarathy, *ibid.* **4**, 555 (1936).
 [16] V. M. Akulin, F. L. Kien, and W. P. Schleich, *Phys. Rev. A* **44**, R1462 (1991).
 [17] M. J. Holland, D. F. Walls, and P. Zoller, *Phys. Rev. Lett.* **67**, 1716 (1991).
 [18] A. M. Herkommer, V. M. Akulin, and W. P. Schleich, *Phys. Rev. Lett.* **69**, 3298 (1992).
 [19] S. Haroche, M. Brune, and J. M. Raimond, *Appl. Phys. B: Photophys. Laser Chem.* **54**, 355 (1992).
 [20] I. Sh. Averbukh, V. M. Akulin, and W. P. Schleich, *Phys. Rev. Lett.* **72**, 437 (1994).
 [21] M. Freyberger and A. M. Herkommer, *Phys. Rev. Lett.* **72**, 1952 (1994).
 [22] P. Domokos, P. Adam, J. Janszky, and A. Zeilinger, *Phys. Rev. Lett.* **77**, 163 (1996).
 [23] R. Walser, J. I. Cirac, and P. Zoller, *Phys. Rev. Lett.* **77**, 2658 (1996).
 [24] C. V. Raman and N. S. Nagendra Nath, *Proc.-Indian Acad. Sci., Sect. A* **2**, 406 (1935); **2**, 413 (1935); **3**, 75 (1936); **3**, 119 (1936); **3**, 459 (1936), and references therein.
 [25] A. Reichelt, E. Storck, and U. Wolff, *Opt. Commun.* **3**, 169 (1971).
 [26] C. J. Hood, M. S. Chapman, T. W. Lynn, and H. J. Kimble, *Phys. Rev. Lett.* **80**, 4157 (1998).
 [27] K. E. Cahill and R. J. Glauber, *Phys. Rev.* **177**, 1857 (1969); **177**, 1882 (1969).
 [28] R. J. Glauber, *Phys. Rev.* **131**, 2766 (1963).
 [29] D. Leibfried, D. M. Meekhof, B. E. King, C. Monroe, W. M. Itano, and D. J. Wineland, *Phys. Rev. Lett.* **77**, 4281 (1996).
 [30] C. Kurtsiefer, T. Pfau, and J. Mlynek, *Nature (London)* **386**, 150 (1997).
 [31] L. G. Lutterbach and L. Davidovich, *Phys. Rev. Lett.* **78**, 2547 (1997).
 [32] J. J. McClelland, R. E. Scholten, E. C. Palm, and R. J. Celotta, *Science* **262**, 877 (1993).
 [33] G. Timp, R. E. Behringer, D. M. Tennant, and J. E. Cunningham, *Phys. Rev. Lett.* **69**, 1636 (1992).
 [34] A. P. Smirnov, *Opt. Spektrosk.* **44**, 359 (1978) [*Opt. Spectrosc.* **44**, 208 (1978)].
 [35] See, for example, Amnon Yariv, *Quantum Electronics*, 3rd ed. (John Wiley & Sons, New York, 1989).
 [36] A. Dulčić, J. H. Eberly, H. Huang, J. Javanainen, and L. Rosso-Franco, *Phys. Rev. Lett.* **56**, 2109 (1986).